

## **Original Research Article**

### **Processing and characterization of PbS nanoparticles by ball milling technique and their applications**

#### **Abstract**

Lead Sulphide (PbS) nanoparticles were processed using ball milling techniques. The processed PbS nanoparticles were characterized using X-ray diffraction (XRD), atomic absorption spectroscopy (AAS), scanning electron microscopy (SEM), UV-visible spectroscopy, energy dispersive analysis (EDAX), and four-point probe. The XRD results of the PbS nanoparticles show peaks at the crystal plane (111), (200), (210), (211) and (320). The average crystallite size of PbS nanoparticles is found to be 51.05 nm. The optical energy band gap of PbS nanoparticles dispersed in ethanol was observed to be 3.98eV and 4.06eV for PbS nanoparticles dispersed in distilled water. The absorbance of PbS nanoparticles shows that the absorbance values were moderate in the UV region but dramatically decreased as they moved towards the visible and near-infrared regions. The EDX analysis shows that PbS nanoparticles is composed of 54.36% Pb, 36.47% C and 9.16% S. The sheet resistance, resistivity, and conductivity were measured and found to be  $1.51 \times 10^7 \Omega/\text{Sq.}$ ,  $3.61 \Omega.\text{cm}$  and  $2.77 \times 10^{-1} (\Omega.\text{cm})^{-1}$  for PbS nanoparticles. PbS nanoparticles are classified as promising materials for various electronics and optoelectronic devices based on the determined properties.

**Keyword:** *Lead sulphide, ball milling technique, X-ray diffraction, surface morphology, electrical*

#### **Introduction**

Lead sulphide (PbS) is an important IV-VI group semiconductor having narrow direct band gap 0.41 eV at room temperature (300 K). Research on PbS nanoparticles are growing on demand because of its exciton Bohr radius which is 18 nm at room temperature. Having high dielectric constant ( $\epsilon_0 = 169$  at 300 K) as well as high carrier mobility leads to PbS nanoparticles exhibits strong quantum size effect despite of having relatively larger size (greater than 10 nm) along with the large band gap (3.2 eV - 4.4 eV) (Vikesland and Wigginton, 2010). As we know the nanoparticles having same order of exciton Bohr radius with larger band gap as comparison to bulk band gap (0.41 eV) leads to quantum confinement and the particles may be termed as

quantum dot (Nabiyouni, *et al.*, 2012). Due to their unique optical properties, till now PbS nanoparticles are tried to apply in optoelectronics devices such as light-emitting diodes, optical switches, IR detectors, photoluminescence, solar cell etc.

Nanoparticles in general are supposed to have nearly half of their atoms contained in top two monolayers which make optical properties highly sensitive to surface morphology (Chander, 2005). In the recent years, nano-sized semiconducting materials have attracted a considerable interest owing to their structural, chemical and physical properties that differs from those of the corresponding bulk materials (Selim *et al.*, 2013) because of the three-dimensional confinement of electrons and holes in a small volume. The number of atoms on the surface is comparable to that inside the particles. Nanoparticles have larger surface-to volume ratio (Saba *et al.*, 2011) and the atoms on the surface are bound by weaker forces because of missing neighbours that leads to high surface reactivity. At the nanoscale, the properties of particles may change in unpredictable ways (Ndukwe and Ekpunobi, 2023).

Synthesis of nanomaterials by a simple, low cost and in high yield has been a great challenge since the very early development of nanoscience. Various bottom and top-down approaches have been developed so far for the commercial production of nanomaterials. Among all top-down approaches, high energy ball milling has been widely exploited for the synthesis of various nanomaterials, nanograins, nanoalloy, nanocomposites and nano-quasicrystalline materials.

PbS nanoparticles (NPs) show strong quantum size effects for relatively large size. Also, their absorption edge can be tuned to anywhere between red to violet covering the entire visible spectrum (Chongad *et al.*, 2016). PbS nanoparticles have been prepared by various techniques but they require sophisticated instruments. Keeping in mind the importance of PbS

nanoparticles development of a simple and economic method of preparation is highly desirable.

In this work, lead sulphide ore were reduced to nano size by mechanical milling technique because when reduced to nanoparticles, they possess interesting structural, optical, and electrical properties which cannot be found in their bulk form.

The processed nanoparticles have been characterized using X-ray diffraction (XRD), atomic absorption spectroscopy (AAS), scanning electron microscopy (SEM), UV-visible spectroscopy, energy dispersive analysis (EDAX), and four-point probe.

## **2.0 Materials and method**

### **2.1 Materials used**

The materials used for this work are as given as follows: Ball mill, Beakers, Volumetric cylinder, Funnel, Filter paper, Magnetic stirrer, Thermometer, Heating mantle

### **2.2 Processing of PbS nanoparticles**

PbS nanoparticles were processed using the ball milling techniques. The Galena (PbS) ores used for this study were collected from Abakaliki, Enyigba mining site in Ebonyi State of Nigeria. The Ores were granulated to nano sizes ranging from 0-100 nanometers using 5kg laboratory ball mill. The following reagents were used in the preparation of the aqua regia for acid digestion of the samples, Hydrochloric (HCL) and nitric acid (HNO<sub>3</sub>), Deionized water.

### **2.3 Sample preparation for AAS analysis**

Procedures

This digestion method used in this work is based on EPA method 3052 and the China National Standard to extract the elements from the soil samples and is not intended for full decomposition of the sample. 2 gram of soil samples were weighed directly into 100 mL polypropylene (PP) reaction vessels. Using the same acids combination as the standard for soil samples digestion, 70% HCl and 30% HNO<sub>3</sub> (all concentrated) were added to each sample. Analytical reagent blanks were also prepared and contained only the acids. The vessels were lightly covered with the lids and placed into the block. The samples were digested at 120 °C for 1h. Following the digestion, the cooled digested sample solutions were diluted to final volume of 100.0 mL deionized water and then filtered. The filtrate solution was ready for analysis. The Atomic Absorption Spectroscopy analysis was performed using a Buck Scientific AAS 211.

## **2.4 Sample preparation for soil electrical conductivity**

### **Procedure**

2 gram of the sample was weighed into a beaker and 50 ml of deionized water was added to cover the soil sample complete. The solution was allowed to shake in a mechanical shaker at 15 rpm for 1 hour to dissolve the soil sample. The EC meter was calibrated according to the manufacturer's instructions using the KCl reference solution to obtain the cell constant. The EC was read and recorded accordingly.

## **2.5 Characterization of PbS nanoparticles**

The morphology of the nanoparticles was examined using a scanning electron microscope (SEM). The crystal lattice and peak intensities was investigated using Bruker D8 Advance XRD with Cu-K $\alpha$  radiation ( $\lambda = 1.5406\text{\AA}$ ) in the range from  $15^\circ$  to  $80^\circ$ . The elemental composition of a samples was performed using Energy Dispersive X-ray analysis. Buck 210/211ATS compact spectrometer was used in the analysis of the concentration of metallic elements in the given sample based on the amount of energy absorbed. The electrical conductivity of the soil samples was determined using electrical conductivity meter. The optical properties of the nanoparticles were investigated using a Shimadzu UV-1800 visible spectrophotometer in the range of 200 to 1100 nm. The electrical characteristics of nanoparticles was examined using an old Jandel four-point probes (model TY242MP) technique.

## **3.0 Results and Discussion**

### **3.1 Atomic Absorption Spectroscopy (AAS) Analysis**

Table 1 shows the concentration of metallic atom present in PbS nanoparticles. According to the AAS analysis, the sample of PbS nanoparticles contains 140g/kg of Pb while also including trace amounts of other metals such minor elements like Iron and Copper.

**Table 1: AAS analysis of PbS nanoparticles**

Elements	PbS Nanoparticles (g/kg)
Lead (Pb)	140.000
Zinc (Zn)	Undetected
Iron (Fe)	0.360
Copper (Cu)	0.003

### 3.2 Soil electrical conductivity

Table.2 shows the soil electrical conductivity PbS nanoparticles using electrical conductivity metre. The EC analysis shows that PbS nanoparticles has an electrical conductivity value of 103.2 ( $\mu\text{S}/\text{cm}$ )

Samples	EC VALUE ( $\mu\text{S}/\text{cm}$ ) @ 28 <sup>o</sup> C
PbS	103.2

**Table 2: Soil electrical conductivity PbS nanoparticles**

### 3.3 Optical analysis of PbS Nanoparticles

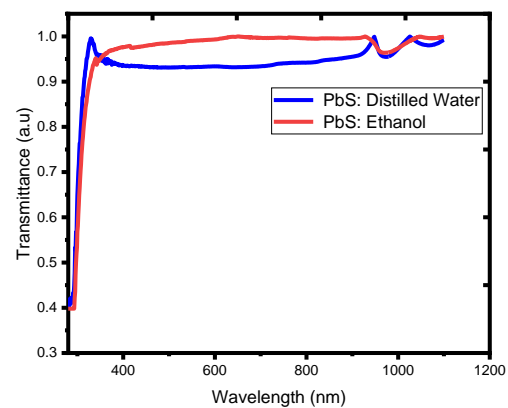
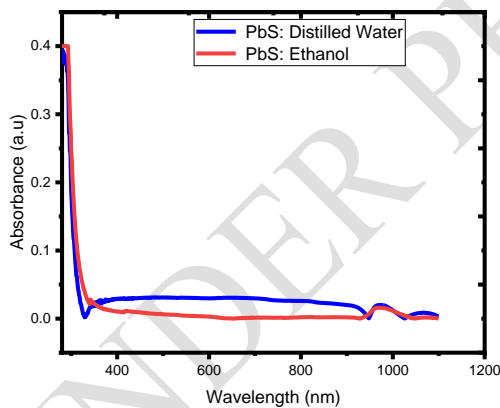
The absorbance result of PbS nanoparticles dispersed in distilled water and ethanol is shown in Figure 1a. When PbS nanoparticles was dispersed in distilled water and ethanol, the absorbance in the UV region of the spectrum was moderate (40%) at wavelengths of 284 nm and 292 nm, before dropping sharply to 1% and 3% respectively. In the visible portion of the spectrum, the PbS nanoparticles dispersed in distilled water showed a slight increase of 2%, which decreased slightly as they proceeded into the NIR region of the spectrum. In the visible spectrum, the ethanol- dispersed PbS nanoparticles showed a shallow pattern that diminished as they proceeded into the NIR range. The PbS nanoparticles exhibited very poor absorption of radiation in the visible region of the electromagnetic spectrum and moderate absorption in the ultraviolet region.

The transmittance of distilled water dispersed PbS nanoparticles increases from 40% to 98% in the UV-visible region of the spectrum, followed by a shallow fall of 4% in the visible area, which increased slightly as they proceeded into the NIR region of the spectrum while the transmittance of ethanol- dispersed PbS nanoparticles increases from 40% to 94% in the UV-visible region of the spectrum, followed by a shallow increase in the visible and NIR region of the spectrum as seen in Figure 1b. The PbS nanoparticles displayed very high transmittance throughout the UV-VIS-NIR region of the electromagnetic spectrum.

As can be seen in Figure 1c, the distilled water dispersed PbS nanoparticles likewise displayed poor reflection of light which decrease from 20% to 1% in the UV region of the spectrum, followed by a sharp increase of 2% in the visible region which decrease slightly as they proceeded into the NIR region while the reflectance of ethanol- dispersed PbS nanoparticles increases from 20% to 2% in the UV-visible region of the spectrum, followed by a shallow decrease in the visible and NIR region of the spectrum. The PbS nanoparticles displayed very poor reflection of light throughout the UV-VIS-NIR region of the electromagnetic spectrum.

Direct band gap of the PbS nanoparticles sample was determined by plotting  $(\alpha h\nu)^2$  versus  $h\nu$  and then extrapolating the straight portion of the Tauc plots as shown in Figure 1d. The value of optical band gap was found to be 3.98eV for PbS nanoparticles dispersed in ethanol and 4.06eV for PbS nanoparticles dispersed in distilled water. This result agrees with several studies on PbS nanoparticles obtained in literatures (Mamiyev *et al.*, 2015; Himadri *et al.*, 2018; Kumar *et al.*, 2009).

It is reported that the band gap of a specific material does not only depend on its structure but the size also has a controlling factor. Once the particle reaches nano-meter size, quantum effects come into play and the effective band gap increases. Increasing bandgap energies of PbS nanoparticles could be evidence of the quantum confinement effect due to decreasing size of structures (Nwauzor *et al.*, 2023; Hamed *et al.*, 2021).



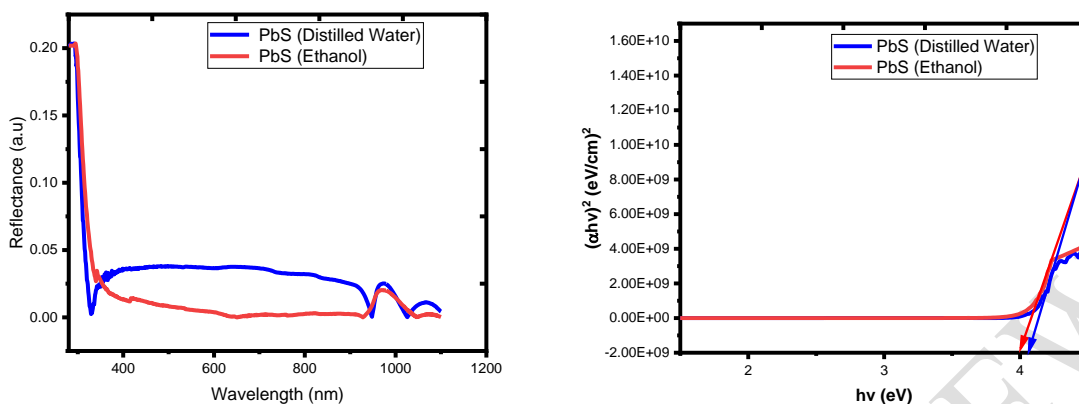


**Figure 1(a) Absorbance spectra of PbS nanoparticles, (b) Transmittance spectra of PbS nanoparticles, (c) Reflectance spectra of PbS nanoparticles, (d) Optical energy bandgap plot of PbS nanoparticles**

### 3.4 Surface morphological investigation of PbS nanoparticles

The SEM characterization of PbS nanoparticles was done at University of Cape town, with Scanning Electron Microscope Carl Zeiss EVO 18 instrument. The topographical images obtained with non-conducting mode with different magnifications are shown in Figure 2.

According to the SEM microstructural investigation, the synthesized PbS contains mainly the grains of PbS particles (crystallite) with regular shape. (Ologundudu *et al.*, 2022).

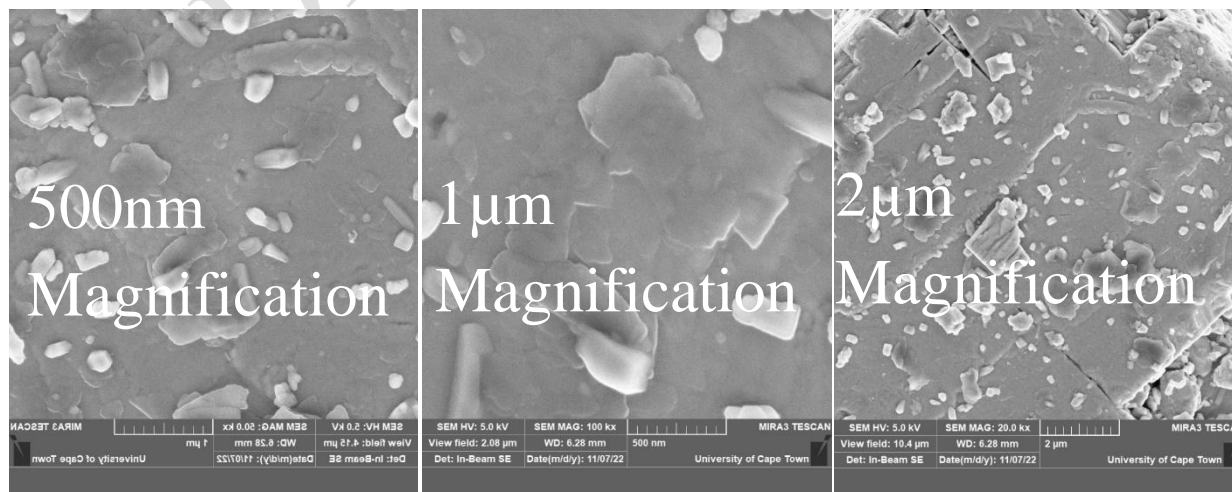


## Figure 2: SEM micrographs of PbS nanoparticles

### 3.5 Elemental Composition of PbS Nanoparticles

Figure 3 shows the analysis of the elemental composition of PbS nanoparticles using Energy dispersive X-ray (EDX). The EDX revealed the compound composition of all the elements it is composed (Dengo *et al.*, 2020; Fang *et al.*, 2011). The energy dispersive X-ray (EDX) analysis of PbS (Table 3) also revealed that the chemical components were predominantly of 54.36% Pb, followed by 36.47% C and 9.16% S.

**Table 3: Atomic weight percentages of constituent elements in EDX spectra**

PbS Nanoparticles	
Element	Atomic Weight (%)
Lead	54.36
Sulfur	9.16
Carbon	36.47

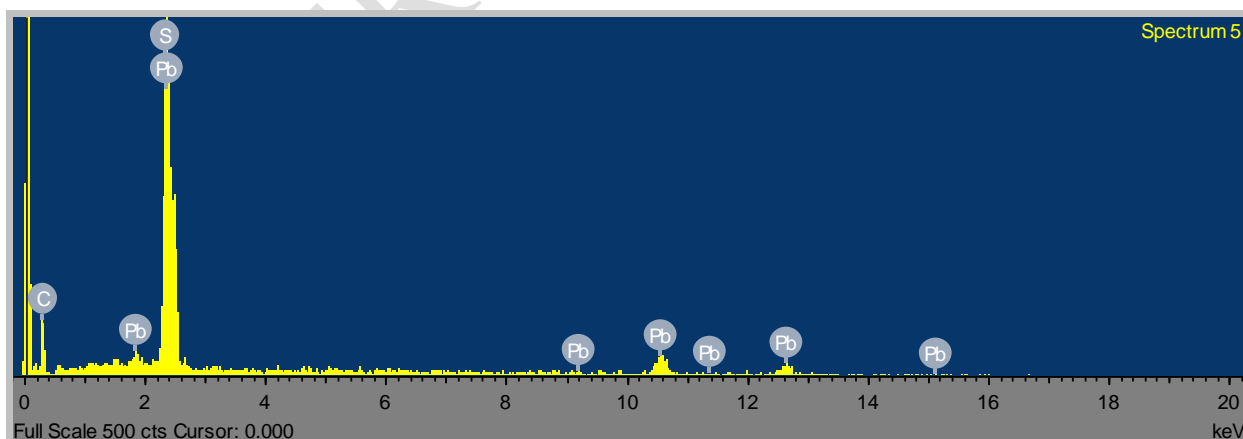


**Figure 3: EDX spectrum of PbS nanoparticles**

### 3.6 Structural analysis of PbS nanoparticles

Structural investigation of PbS nanoparticles was carried out using X-ray powder diffractometer (XRD) with a Cu-K $\alpha$  radiation source ( $\lambda = 1.5406 \text{ \AA}$ ). Figure 4 the PbS nanoparticles XRD diffraction pattern. Distinct peaks of the PbS nanoparticles were observed at  $21.65^\circ$ ,  $23.11^\circ$ ,  $23.77^\circ$ ,  $28.70^\circ$ ,  $32.78^\circ$  and  $47.04^\circ$  corresponding to (111), (200), (210), (211), and (320) crystallographic planes. Some XRD peaks are left out without indexing because they might have been created by contaminants in the sample. The broadening of peaks in the XRD pattern indicates the nanocrystalline nature of the samples. (Dengoet *et al.*, 2020; Chaudhary *et al.*, 2016). The average crystallite sizes were calculated using the Debye-Scherrer equation (Onu *et al.*, 2023; Ebnalwaled *et al.*, 2017; Yimin *et al.*, 2018). The average crystallite size of PbS nanoparticles was found to be 51.05 nm. The material's computed structural characteristics are shown in Table 4.

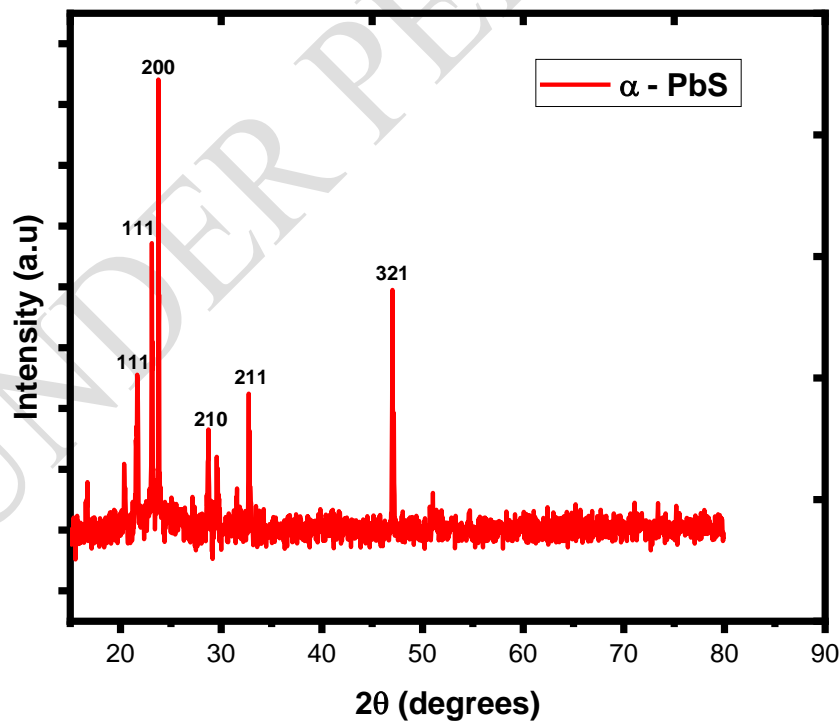


**Figure 4: X-Ray Diffraction pattern for PbS nanoparticles**

**Table 4 Structural parameters for PbS nanoparticles**

<b>2θ (degree )</b>	<b>Spacing d(Å)</b>	<b>Lattice constant a (Å)</b>	<b>FWHM, β</b>	<b>hkl</b>	<b>Crystallite Size, D (nm)</b>	<b>Dislocation density, δ × 10<sup>3</sup> (nm)<sup>-2</sup></b>
21.65	4.101	7.104	0.235	111	34.440	0.843
23.11	3.845	6.660	0.144	111	56.197	0.317
23.77	3.741	7.482	0.096	200	84.214	0.141
28.70	3.108	6.949	0.169	210	48.496	0.425
32.78	2.730	6.687	0.217	211	38.208	0.685
47.04	1.930	7.222	0.193	321	44.864	0.497

### **3.6 Electrical Properties**

Using the four-point probe technique, the electrical (I-V) measurement PbS nanoparticles was determined. The nanoparticles were applied to a glass substrate before the electrical investigation was performed. Figure 5 shows the average current and the related voltage. We noticed that the current passing through the film rises linearly as the electrode's voltage increases. This suggests that the film has a higher conductivity, which could assist in the production of solar cells with a higher frequency fabrication (Thirumavalavan *et al.*, 2015). The average current and voltage of PbS thin film were found to be  $3.85 \times 10^{-8}$  A and  $12.8 \times 10^{-2}$  V.

The resistivity ( $\rho$ ) was estimated using the relation relation (Emegha *et al.*, 2019);

$$\rho = \frac{\pi}{ln2} \left( \frac{V}{I} \right) \times W \quad (1)$$

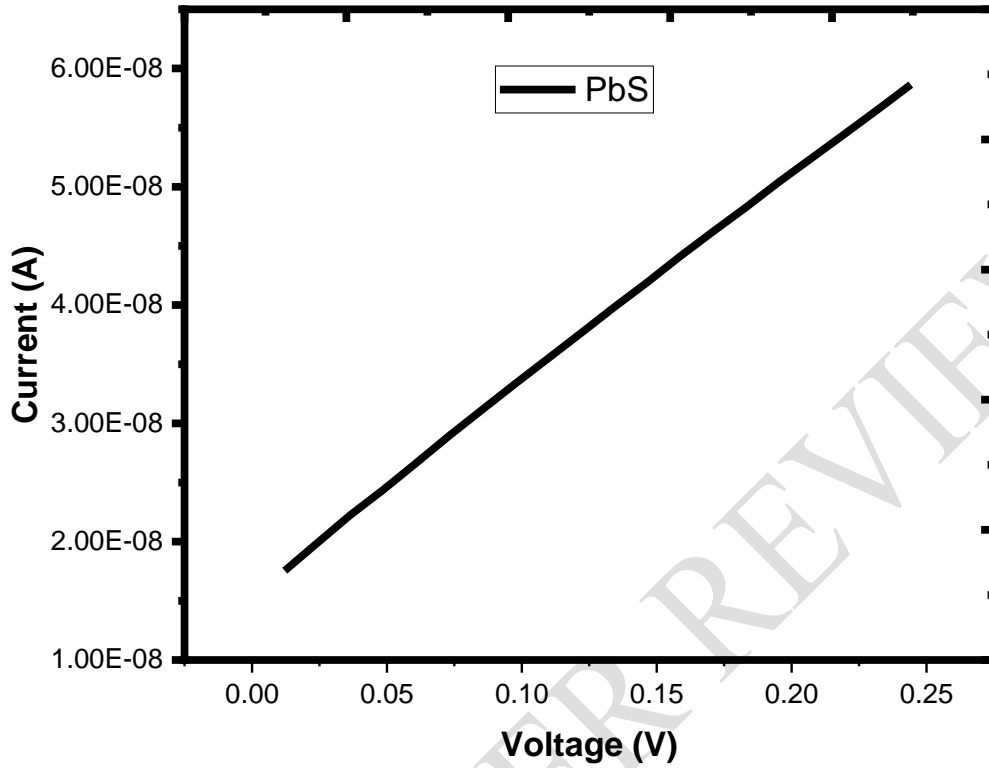


Figure 5: I-V characteristic of PbS nanoparticles

Where  $W$  is the film thickness, whose value 239.85 nm for PbS nanoparticles on the glass substrate.  $V$  and  $I$  are the average voltage and current of the film respectively. The reciprocal of the resistivity was taken as the conductivity ( $\sigma$ ) of the film.

$$\sigma = \frac{1}{\rho} \quad (2)$$

from the values of resistivity ( $\rho$ ) and thickness ( $W$ ), the sheet resistance ( $R_s$ ) can be determined as

$$R_s = \frac{\rho}{W} \quad (3)$$

The sheet resistance for PbS was found to be  $1.51 \times 10^7 \Omega/\text{Sq.}$ , the resistivity was calculated to be  $3.61 \Omega.\text{cm}$  and the conductivity was also calculated to be  $2.77 \times 10^{-1} (\Omega.\text{cm})^{-1}$ . The electrical conductivity value falls within the magnitude of  $10^{-13}$  to  $10^2$  reported for

semiconducting thin films in literature (Okafor *et al.*, 2014), suggesting that the deposited film is conductive in nature. The observed high resistive value of the film indicates that it could find application as semiconducting sensors.

## Conclusions

Lead sulphide (PbS) nanoparticles had been successfully processed utilizing a mechanical milling technique. The processed PbS nanoparticles were characterized using X-ray diffraction (XRD), atomic absorption spectroscopy (AAS), scanning electron microscopy (SEM) and UV-visible spectroscopy, energy dispersive analysis (EDAX), to study their structural, concentration of elements in the given sample, morphological, optical properties and elemental composition of the samples.

The PbS nanoparticles' XRD measurements reveal peaks at the crystal plane (111), (200), (210), (211) and (320). The average crystallite size of PbS nanoparticles was found to be 51.05 nm. The optical energy band gap was found to be 3.98 eV for PbS nanoparticles dispersed in ethanol and 4.06 eV for PbS nanoparticles dispersed in distilled water. The absorbance of PbS nanoparticles shows that the absorbance values were moderate in the UV region but dramatically decreased as they moved towards the visible and near-infrared regions. The PbS nanoparticles displayed very high transmittance and very poor reflection of light of throughout the UV-VIS-NIR region of the electromagnetic spectrum

PbS nanoparticles contain 54.36% Pb, 36.47% C and 9.16% S according to elemental analysis of their composition. The sheet resistance, resistivity, and conductivity were measured and found to be  $1.51 \times 10^7 \Omega/\text{Sq.}$ ,  $3.61 \Omega.\text{cm}$  and  $2.77 \times 10^{-1} (\Omega.\text{cm})^{-1}$ , respectively.

## References

Chander, H. (2005). Development of nanophosphors—A review. *Materials Science and Engineering: R: Reports*, 49(5), 113-155

- Chaudhary, M. D., Patel, J. C., & Chaudhari, J. M. (2016). Study of PbS nanoparticles synthesized by chemical route. *Int. J. Inno. Res. Mult. Field*, 2(12), 263-266.
- Chongad, L. S., Sharma, A., Banerjee, M., & Jain, A. (2016, October). Synthesis of lead sulfide nanoparticles by chemical precipitation method. In *Journal of Physics: Conference Series* (Vol. 755, No. 1, p. 012032). IOP Publishing.
- Dengo, N., Vittadini, A., Natile, M. M., & Gross, S. (2020). In-depth study of ZnS nanoparticle surface properties with a combined experimental and theoretical approach. *The Journal of Physical Chemistry C*, 124(14), 7777-7789.
- Ebnalwaled, A. A., Essai, M. H., Hasaneen, B. M., & Mansour, H. E. (2017). Facile and surfactant-free hydrothermal synthesis of PbS nanoparticles: the role of hydrothermal reaction time. *Journal of Materials Science: Materials in Electronics*, 28(2), 1958-1965.
- Emegha, J. O., Elete, E. D., Efe, F. O. O., & Adebisi, A. C. (2019). Optical and electrical properties of semiconducting ZnS thin film prepared by chemical bath deposition technique. *catalysis*, 3, 4.
- Hamed, Z. H., Ahmed, K. E. A., & Elsheikh, H. A. (2021). Synthesis and characterization of ZnS nanoparticles by chemical precipitation method. *Aswan University Journal of Environmental Studies*, 2(2), 147-154.
- Himadri, D., Pranayee, D., & Kumar, S. K. (2018). Synthesis of pbs nanoparticles and its potential as a biosensor based on memristic properties. *Journal of Nanoscience and Technology*, 500-502.
- Kumar, D., Agarwal, G., Tripathi, B., Vyas, D., & Kulshrestha, V. (2009). Characterization of PbS nanoparticles synthesized by chemical bath deposition. *Journal of Alloys and Compounds*, 484(1-2), 463-466.
- Mamiyev, Z. Q., & Balayeva, N. O. (2015). Preparation and optical studies of PbS nanoparticles. *Optical Materials*, 46, 522-525.
- Nabiyouni, G., Moghimi, E., Hedayati, K., & Jalajerdi, R. (2012). Room temperature synthesis of lead sulfide nanoparticles. *Main Group Metal Chemistry*, 35(5-6), 173-178.
- Ndukwe, F., & Ekpunobi, A. (2023). Processing and Characterization of Limestone Nanoparticles. *American Journal of Physical Sciences*, 1(1), 63-70.
- Nwauzor, J. N., Ekpunobi, A. J., & Babalola, A. D. (2023). Processing and Characterization of Iron Oxide Nanoparticle Produced by Ball Milling Technique. *Asian Journal of Physical and Chemical Sciences*, 11(1), 27-35.
- Okafor, P. C., Ekpunobi, A. J., & Ekwo, P. A. (2014). Effect of manganese percentage doping on thickness and conductivity of zinc sulphide nanofilms prepared by electrodeposition method. *International Journal of Science and Research (IJSR)*, 4, 2275-2279.
- Ologundudu, S. K., Ekpunobi, A. J., & Ikhioya, I. L. (2022). Synthesis and Characterization of ZnS Nanoparticles by Ball Milling Technique.
- Onu, C. P., Ekpunobi, A. J., Okafor, C. E., & Ozobialu, L. A. (2023). Optical Properties of Monazite Nanoparticles Prepared Via Ball Milling. *Asian Journal of Research and Reviews in Physics*, 7(4), 17-29.

- Saba, S., Bera, K & Jana, P.C. (2011). Growth time dependence of size of nanoparticles of ZnS, *International Journal of Soft Computing and Engineering (IJSCE)*. Vol. 1, Issue 5. pp 23.
- Selim, H., Khalil, M. M. H., Al-Kotb, M. S., Kotkata, M. F., & Amer, H. H. (2013). Synthesis and structural characterization of ZnS quantum dots. *Journal of Radiation Research and Applied Sciences*, 6(1), 89-103.
- Thirumavalavan, S., Mani, K., & Sagadevan, S. (2015). Studies on structural, surface morphology and optical properties of zinc sulphide (ZnS) thin films prepared by chemical bath deposition. *International Journal of Physical Sciences*, 10(6), 204-209.
- Vikesland, P. J., & Wigginton, K. R. (2010). Nanomaterial enabled biosensors for pathogen monitoring-a review. *Environmental science & technology*, 44(10), 3656-3669
- Yimin, D., Jiaqi, Z., Danyang, L., Lanli, N., Liling, Z., Yi, Z., & Xiaohong, Z. (2018). Preparation of Congo red functionalized Fe<sub>3</sub>O<sub>4</sub>@ SiO<sub>2</sub> nanoparticle and its application for the removal of methylene blue. *Colloids and Surfaces A: Physicochemical and Engineering Aspects*, 550, 90-98.